

000 001 002 003 004 005 006 007 008 009 010 011 012 013 014 015 016 017 018 019 020 021 022 023 024 025 026 027 028 029 030 031 032 033 034 035 036 037 038 039 040 041 042 043 044 045 046 047 048 049 050 051 052 053 THE MECHANISTIC EMERGENCE OF SYMBOL GROUNDING IN LANGUAGE MODELS

Anonymous authors

Paper under double-blind review

ABSTRACT

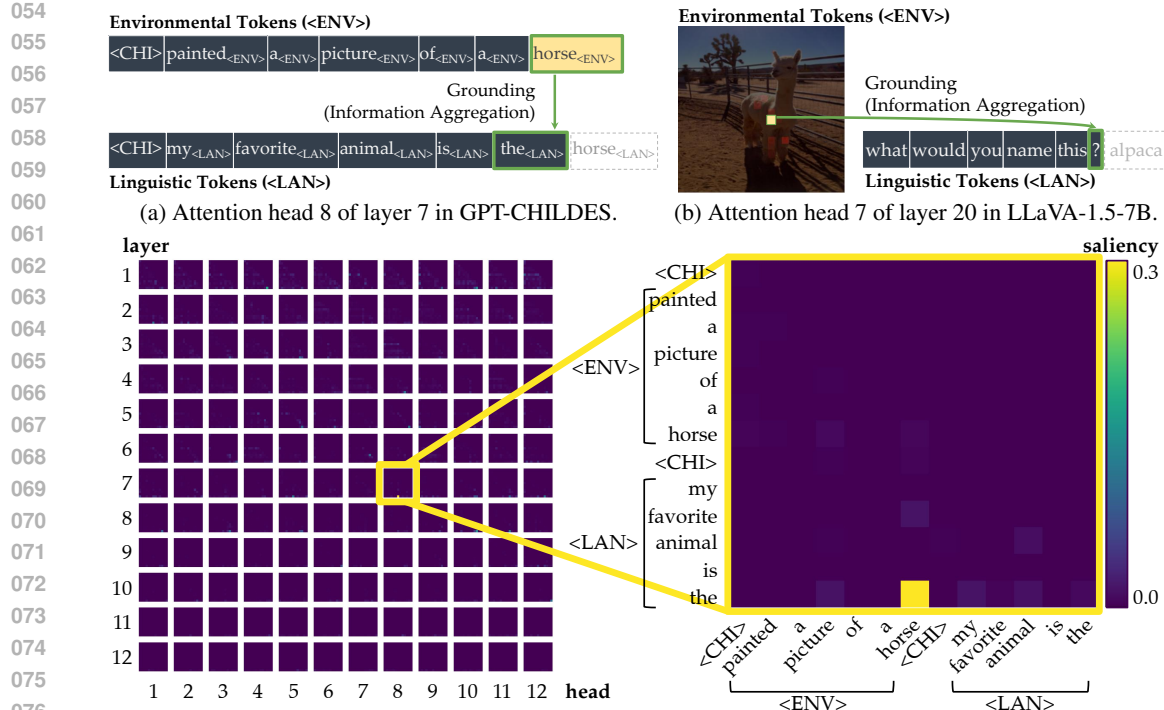
Symbol grounding (Harnad, 1990) describes how symbols such as words acquire their meanings by connecting to real-world sensorimotor experiences. Recent work has shown preliminary evidence that grounding may emerge in (vision-)language models trained at scale without using explicit grounding objectives. Yet, the specific loci of this emergence and the mechanisms that drive it remain largely unexplored. To address this problem, we introduce a controlled evaluation framework that systematically traces how symbol grounding arises within the internal computations through mechanistic and causal analysis. Our findings show that grounding concentrates in middle-layer computations and is implemented through the aggregate mechanism, where attention heads aggregate the environmental ground to support the prediction of linguistic forms. This phenomenon replicates in multimodal dialogue and across architectures (Transformers and state-space models), but not in unidirectional LSTMs. Our results provide behavioral and mechanistic evidence that symbol grounding can emerge in language models, with practical implications for predicting and potentially controlling the reliability of generation.

1 INTRODUCTION

Symbol grounding (Harnad, 1990) refers to the problem of how abstract and discrete symbols, such as words, acquire meaning by connecting to perceptual or sensorimotor experiences. Extending to the context of multimodal machine learning, grounding has been leveraged as an explicit pre-training objective for vision-language models (VLMs), by explicitly connecting linguistic units to the world that gives language meanings (Li et al., 2022; Ma et al., 2023). Through supervised fine-tuning with grounding signals, such as entity-phrase mappings, modern VLMs have achieved fine-grained understanding at both region (You et al., 2024; Peng et al., 2024; Wang et al., 2024) and pixel (Zhang et al., 2024b; Rasheed et al., 2024; Zhang et al., 2024a) levels.

With the rising of powerful autoregressive language models (LMs; OpenAI, 2024; Anthropic, 2024; Comanici et al., 2025, *inter alia*) and their VLM extensions, there is growing interest in identifying and interpreting their emergent capabilities. Recent work has shown preliminary correlational evidence that grounding may emerge in LLMs (Sabet et al., 2020; Shi et al., 2021; Wu et al., 2025) and VLMs (Cao et al., 2024; Bousselham et al., 2024; Schnaus et al., 2025) trained at scale, even when solely optimized with the simple next-token prediction objective. However, the potential underlying mechanisms that lead to such an emergence are not well understood. To address this limitation, our work seeks to understand the emergence of symbol grounding in LMs, causally and mechanistically tracing how symbol grounding arises within the internal computations.

We begin by constructing a minimal testbed, motivated by the annotations provided in the CHILDES corpora (MacWhinney, 2000), where child–caregiver interactions provide cognitively plausible contexts for studying symbol grounding alongside verbal utterances. In our framework, each word is represented in two distinct forms: one token that appears in non-verbal scene descriptions (e.g., a *box* in the environment) and another that appears in spoken utterances (e.g., *box* in dialogue). We refer to these as environmental tokens ($\langle \text{ENV} \rangle$) and linguistic tokens ($\langle \text{LAN} \rangle$), respectively. A deliberately simple word-level tokenizer assigns separate vocabulary entries to each form, ensuring that they are treated as entirely different tokens by the language model. This framework enforces a structural separation between scenes and symbols, preventing correspondences from being reduced to trivial token identity. Under this setup, we can evaluate whether a model trained from scratch is able to predict the linguistic form from its environmental counterpart.



(c) Left: saliency over tokens of each head in each layer for the prompt $\langle CHI \rangle$ painted_(ENV) a_(ENV) picture_(ENV) of_(ENV) a_(ENV) horse_(ENV) $\langle CHI \rangle$ my_(LAN) favorite_(LAN) animal_(LAN) is_(LAN) the_(LAN). Right: among all, only one of them (head 8 of layer 7) is identified as an aggregate head, where information flows from horse_(ENV) to the current position, encouraging the model to predict horse_(LAN) as the next token.

Figure 1: Illustration of the symbol grounding mechanism through information aggregation. Lighter colors denote more salient attention, quantified by saliency scores, i.e., gradient \times attention contributions to the loss (Wang et al., 2023). When predicting the next token, aggregate heads (Bick et al., 2025) emerge to exclusively link environmental tokens (visual or situational context; $\langle \text{ENV} \rangle$) to linguistic tokens (words in text; $\langle \text{LAN} \rangle$). These heads provide a mechanistic pathway for symbol grounding by mapping external environmental evidence into its linguistic form.

We quantify the level of grounding using surprisal: specifically, we compare how easily the model predicts a linguistic token ($\langle \text{LAN} \rangle$) when its matching environmental token ($\langle \text{ENV} \rangle$) is present versus when unrelated cues are given instead. A lower surprisal in the former condition indicates that the model has learned to align environmental grounds with linguistic forms. We find that LMs do learn to ground: the presence of environmental tokens consistently reduces surprisal for their linguistic counterparts, in a way that simple co-occurrence statistics cannot fully explain. To study the underlying mechanisms, we apply saliency analysis (Wang et al., 2023) and the tuned lens (Belrose et al., 2023), which converge on the result that grounding relations are concentrated in the middle layers of the network. Further analysis of attention heads reveals patterns consistent with the aggregate mechanism (Bick et al., 2025), where attention heads support the prediction of linguistic forms by retrieving their environmental grounds in the context.

Finally, we demonstrate that these findings generalize beyond the minimal CHILDES data and Transformer models. They appear in a multimodal setting with the Visual Dialog dataset (Das et al., 2017), and in state-space models (SSMs) such as Mamba-2 (Dao & Gu, 2024). In contrast, we do not observe grounding in unidirectional LSTMs, consistently with their sequential state compression and lack of content-addressable retrieval. Taken together, our results show that symbol grounding can mechanistically emerge in autoregressive LMs, while also delineating the architectural conditions under which it can arise.

2 RELATED WORK

Language grounding. Referential grounding has long been framed as the lexicon acquisition problem: how words map to referents in the world (Harnad 1990; Gleitman & Landau 1994;

Clark, 1995). Early work focused on word-to-symbol mappings, designing learning mechanisms that simulate children’s lexical acquisition and explain psycholinguistic phenomena (Siskind, 1996; Regier, 2005; Goodman et al., 2007; Fazly et al., 2010). Subsequent studies incorporated visual grounding, first by aligning words with object categories (Roy & Pentland, 2002; Yu, 2005; Xu & Tenenbaum, 2007; Yu & Ballard, 2007; Yu & Siskind, 2013), and later by mapping words to richer visual features (Qu & Chai, 2010; Mao et al., 2019; 2021; Pratt et al., 2020). More recently, large-scale VLMs trained with paired text–image supervision have advanced grounding to finer levels of granularity, achieving region-level (Li et al., 2022; Ma et al., 2023; Chen et al., 2023; You et al., 2024; Wang et al., 2024) and pixel-level (Xia et al., 2024; Rasheed et al., 2024; Zhang et al., 2024b) grounding, with strong performance on referring expression comprehension (Chen et al., 2024a).

Recent work suggests that grounding emerges as a property of VLMs trained without explicit supervision, with evidence drawn from attention-based spatial localization (Cao et al., 2024; Bousselham et al., 2024) and cross-modal geometric correspondences (Schnaus et al., 2025). However, all prior work focused exclusively on static final-stage models, overlooking the training trajectory, a crucial aspect for understanding when and how grounding emerges. In addition, existing work has framed grounding through correlations between visual and textual signals, diverging from the definition by Harnad (1990), which emphasizes causal links from symbols to meanings. To address these issues, we systematically examine learning dynamics throughout the training process, applying causal interventions to probe model internals and introducing control groups to enable rigorous comparison.

Emergent capabilities and learning dynamics of LMs. A central debate concerns whether larger language models exhibit genuinely new behaviors: Wei et al. (2022) highlight abrupt improvements in tasks, whereas later studies argue such effects are artifacts of thresholds or in-context learning dynamics (Schaeffer et al., 2023; Lu et al., 2023). Beyond end performance, developmental analyses show that models acquire linguistic abilities in systematic though heterogeneous orders with variability across runs and checkpoints (Sellam et al., 2021; Blevins et al., 2022; Biderman et al., 2023; Xia et al., 2023; van der Wal et al., 2025). Psychology-inspired perspectives further emphasize controlled experimentation to assess these behaviors (Hagendorff, 2023), and comparative studies reveal both parallels and divergences between machine and human language learning (Chang & Bergen, 2022; Evanson et al., 2023; Chang et al., 2024; Ma et al., 2025). At a finer granularity, hidden-loss analyses identify phase-like transitions (Kangaslahti et al., 2025), while distributional studies attribute emergence to stochastic differences across training seeds (Zhao et al., 2025). Together, emergent abilities are not sharp discontinuities but probabilistic outcomes of developmental learning dynamics. Following this line of work, we present a probability- and model internals-based analysis of how symbol grounding emerges during language model training.

Mechanistic interpretability of LMs. Mechanistic interpretability has largely focused on attention heads in Transformers (Elhage et al., 2021; Olsson et al., 2022; Meng et al., 2023; Bietti et al., 2023; Lieberum et al., 2023; Wu et al., 2024). A central line of work established that *induction heads* emerge to support in-context learning (ICL; Elhage et al., 2021; Olsson et al., 2022), with follow-up studies tracing their training dynamics (Bietti et al., 2023) and mapping factual recall circuits (Meng et al., 2023). At larger scales, Lieberum et al. (2023) identified specialized *content-gatherer* and *correct-letter* heads, and Wu et al. (2024) showed that a sparse set of *retrieval heads* is critical for reasoning and long-context performance. Relatedly, Wang et al. (2023) demonstrated that label words in demonstrations act as *anchors*: early layers gather semantic information into these tokens, which later guide prediction. Based on these insights, Bick et al. (2025) proposed that retrieval is implemented through a coordinated *gather-and-aggregate (G&A)* mechanism: some heads collect content from relevant tokens, while others aggregate it at the prediction position. Other studies extended this line of work by analyzing failure modes and training dynamics (Wiegreffe et al., 2025) and contrasting retrieval mechanisms in Transformers and SSMs (Arora et al., 2025). Whereas prior analyses typically investigate ICL with repeated syntactic or symbolic formats, our setup requires referential alignment between linguistic forms and their environmental contexts, providing a complementary testbed for naturalistic language grounding.

3 METHOD

3.1 DATASET AND TOKENIZATION

To capture the emergent grounding from multimodal interactions, we design a minimal testbed with a custom word-level tokenizer, in which every lexical item is represented in two corresponding forms:

162 one token that appears in non-verbal descriptions (e.g., a *book* in the scene description) and another
 163 that appears in utterances (e.g., *book* in speech). We refer to these by environmental ($\langle \text{ENV} \rangle$) and
 164 linguistic tokens ($\langle \text{LAN} \rangle$), respectively. For instance, $\text{book}_{\langle \text{ENV} \rangle}$ and $\text{book}_{\langle \text{LAN} \rangle}$ are treated as distinct
 165 tokens with separate integer indices; that is, the tokenization provides no explicit signal that these
 166 tokens are related, so any correspondence between them must be learned during training rather than
 167 inherited from their surface form. We instantiate this framework in three datasets, ranging from
 168 child-directed speech transcripts to image-based dialogue.

169 **Child-directed speech.** The Child Language Data Exchange System (CHILDES; MacWhinney,
 170 2000) provides transcripts enriched with environmental annotations.¹ We use the spoken utterances
 171 as the linguistic tokens ($\langle \text{LAN} \rangle$) and the environmental descriptions as the environment tokens ($\langle \text{ENV} \rangle$).
 172 The environmental context is drawn from three annotation types:

- 173 • **Local events:** simple events, pauses, long events, or remarks interleaved with the transcripts.
- 174 • **Action tiers:** actions performed by the speaker or listener (e.g., %act: runs to toy box). These
 175 also include cases where an action replaces speech (e.g., 0 [% kicks the ball]).
- 176 • **Situational tiers:** situational information tied to utterances or to larger contexts (e.g., %sit: dog
 177 is barking).

178 **Caption-grounded dialogue.** The Visual Dialog dataset (Das et al., 2017) pairs MSCOCO im-
 179 ages (Lin et al., 2014) with sequential question-answering based multi-turn dialogues that exchange
 180 information about each image. Our setup uses MSCOCO captions as the environmental tokens ($\langle \text{ENV} \rangle$)
 181 and the dialogue turns form the linguistic tokens ($\langle \text{LAN} \rangle$). In this pseudo cross-modal setting, textual
 182 descriptions of visual scenes ground natural conversational interaction. Compared to CHILDES, this
 183 setup introduces richer semantics and longer utterances, while still using text-based inputs for both
 184 token types, thereby offering a stepping stone toward grounding in fully visual contexts.

185 **Image-grounded dialogue.** To move beyond textual proxies, we consider an image-grounded
 186 dialogue setup, using the same dataset as the caption-grounded dialogue setting. Here, a frozen
 187 vision transformer (ViT; Dosovitskiy et al., 2020) directly tokenizes each RGB image into patch
 188 embeddings, with each embedding treated as an $\langle \text{ENV} \rangle$ token, analogously to the visual tokens in
 189 modern VLMs. We use DINOv2 (Oquab et al., 2024) as our ViT tokenizer, as it is trained purely
 190 on vision data without auxiliary text supervision (in contrast to models like CLIP; Radford et al.,
 191 2021), thereby ensuring that environmental tokens capture only visual information. The linguistic
 192 tokens ($\langle \text{LAN} \rangle$) remain unchanged from the caption-grounded dialogue setting, resulting in a realistic
 193 multimodal interaction where conversational utterances are grounded directly in visual input.

194 3.2 EVALUATION PROTOCOL

195 We assess symbol grounding with a contrastive test that asks whether a model assigns a higher proba-
 196 bility to the correct linguistic token when the matching environmental token is in context, following
 197 the idea of priming in psychology. This evaluation applies uniformly across datasets (Table 1): in
 198 CHILDES and caption-grounded dialogue, environmental priming comes from descriptive contexts;
 199 in image-grounded dialogue, from ViT-derived visual tokens. We compare the following conditions:

- 200 • **Match (experimental condition):** The context contains the corresponding $\langle \text{ENV} \rangle$ token for the
 201 target word, and the model is expected to predict its $\langle \text{LAN} \rangle$ counterpart.
- 202 • **Mismatch (control condition):** The context is replaced with a different $\langle \text{ENV} \rangle$ token. The model
 203 remains tasked with predicting the same $\langle \text{LAN} \rangle$ token; however, in the absence of corresponding
 204 environmental cues, its performance is expected to be no better than chance.

205 For example (first row in Table 1), when evaluating the word $\text{book}_{\langle \text{LAN} \rangle}$, the input context is

$$\langle \text{CHI} \rangle \text{ asked}_{\langle \text{ENV} \rangle} \text{ for}_{\langle \text{ENV} \rangle} \text{ a}_{\langle \text{ENV} \rangle} \text{ new}_{\langle \text{ENV} \rangle} \text{ book}_{\langle \text{ENV} \rangle} \langle \text{CHI} \rangle \text{ I}_{\langle \text{LAN} \rangle} \text{ love}_{\langle \text{LAN} \rangle} \text{ this}_{\langle \text{LAN} \rangle} \text{ _____}, \quad (1)$$

206 where the model is expected to predict $\text{book}_{\langle \text{LAN} \rangle}$ for the blank, and the role token $\langle \text{CHI} \rangle$ indicates the
 207 involved speaker or actor’s role being a child. In the control (mismatch) condition, the environmental
 208 token $\text{box}_{\langle \text{ENV} \rangle}$ is replaced by another valid noun such as $\text{toy}_{\langle \text{ENV} \rangle}$.

209 **Context templates.** For a target word v with linguistic token $v_{\langle \text{LAN} \rangle}$ and environmental token $v_{\langle \text{ENV} \rangle}$,
 210 we denote \bar{C}_v as a set of context templates of v . For example, when $v = \text{book}$, a $\bar{c} \in \bar{C}_v$ can be

$$\langle \text{CHI} \rangle \text{ asked}_{\langle \text{ENV} \rangle} \text{ for}_{\langle \text{ENV} \rangle} \text{ a}_{\langle \text{ENV} \rangle} \text{ new}_{\langle \text{ENV} \rangle} \text{ [FILLER]} \langle \text{CHI} \rangle \text{ I}_{\langle \text{LAN} \rangle} \text{ love}_{\langle \text{LAN} \rangle} \text{ _____}, \quad (2)$$

211 ¹See the manual for data usage: <https://talkbank.org/0info/manuals/CHAT.pdf>

216 Table 1: Training and test examples across datasets with target word *book*. The training examples
 217 combine environmental tokens ($\langle \text{ENV} \rangle$; shaded) with linguistic tokens ($\langle \text{LAN} \rangle$). Test examples are
 218 constructed with either matched (*book*) or mismatched (*toy*) environmental contexts, paired with
 219 corresponding linguistic prompts. Note that in child-directed speech and caption-grounded dialogue,
 220 $\text{book}_{\langle \text{ENV} \rangle}$ and $\text{book}_{\langle \text{LAN} \rangle}$ are two distinct tokens received by LMs.
 221

Dataset	Training Example		Test Example		
	$\langle \text{ENV} \rangle$	$\langle \text{LAN} \rangle$	$\langle \text{ENV} \rangle$ Match	$\langle \text{ENV} \rangle$ Mismatch	$\langle \text{LAN} \rangle$
Child-Directed Speech	$\langle \text{CHI} \rangle$ takes <i>book</i> from mother	$\langle \text{CHI} \rangle$ what's that $\langle \text{MOT} \rangle$ a <i>book</i> in it ...	$\langle \text{CHI} \rangle$ asked for a new <i>book</i>	$\langle \text{CHI} \rangle$ asked for a new <i>toy</i>	$\langle \text{CHI} \rangle$ I love this
Caption-Grounded Dialogue	<i>a dog appears to be reading a book with a full bookshelf behind</i>	$\langle \text{Q} \rangle$ can you tell what <i>book</i> it's reading $\langle \text{A} \rangle$ the marriage of true minds by stephen evans	<i>this is a book</i>	<i>this is a toy</i>	$\langle \text{Q} \rangle$ can you name this object $\langle \text{A} \rangle$
Image-Grounded Dialogue		$\langle \text{Q} \rangle$ can you tell what <i>book</i> it's reading $\langle \text{A} \rangle$ the marriage of true minds by stephen evans			what do we have here?

231 where $[\text{FILLER}]$ is to be replaced with an environmental token, and the blank indicates the expected
 232 prediction as in Eq. (1). In the match condition, the context $\bar{c}(v)$ is constructed by replacing $[\text{FILLER}]$
 233 with $v_{\langle \text{ENV} \rangle}$ in \bar{c} . In the mismatch condition, the context $\bar{c}(u)$ uses $u_{\langle \text{ENV} \rangle}$ ($u \neq v$) as the filler, while
 234 the prediction target remains $v_{\langle \text{LAN} \rangle}$.
 235

236 For the choices of v and u , we construct the vocabulary V with 100 nouns from the MacArthur–Bates
 237 Communicative Development Inventories (Fenson et al., 2006) that occur frequently in our corpus.
 238 Each word serves once as the target, with the remaining $M = 99$ used to construct mismatched
 239 conditions. For each word, we create $N = 10$ context templates, which contain both $\langle \text{ENV} \rangle$ and $\langle \text{LAN} \rangle$
 240 tokens. Details of the vocabulary and context template construction can be found in the Appendix A.
 241

242 **Grounding information gain.** Following prior work, we evaluate how well an LM learns a word
 243 using the mean surprisal over instances. The surprisal of a word w given a context c is defined
 244 as $s_{\theta}(w | c) = -\log P_{\theta}(w | c)$, where $P_{\theta}(w | c)$ denotes the probability, under an LM parameterized by θ ,
 245 that the next word is w conditioned on the context c . Here, $s_{\theta}(w | c)$ quantifies the unexpectedness of predicting w , or the pointwise information carried by w conditioned on the context.
 246

247 The *grounding information gain* $G_{\theta}(v)$ for v is defined as
 248

$$249 G_{\theta}(v) = \frac{1}{N} \sum_{n=1}^N \left(\frac{1}{M} \sum_{u \neq v}^M \left[s_{\theta}(v_{\langle \text{LAN} \rangle} | \bar{c}_n(u_{\langle \text{ENV} \rangle})) - s_{\theta}(v_{\langle \text{LAN} \rangle} | \bar{c}_n(v_{\langle \text{ENV} \rangle})) \right] \right).$$

250 This is a sample-based estimation of the expected log-likelihood ratio between the match and
 251 mismatch conditions

$$252 G_{\theta}(v) = \mathbb{E}_{c,u} \left[\log \frac{P_{\theta}(v_{\langle \text{LAN} \rangle} | c, v_{\langle \text{ENV} \rangle})}{P_{\theta}(v_{\langle \text{LAN} \rangle} | c, u_{\langle \text{ENV} \rangle})} \right],$$

253 which quantifies how much more information the matched ground provides for predicting the linguistic
 254 form, compared to a mismatched one. A positive $G_{\theta}(v)$ indicates that the matched environmental
 255 token increases the predictability of its linguistic form. We report $G_{\theta} = \frac{1}{|V|} \sum_{v \in V} G_{\theta}(v)$, and track
 256 $G_{\theta(t)}$ across training steps t to analyze how grounding emerges over time.
 257

258 3.3 MODEL TRAINING

259 We train LMs from random initialization, ensuring that no prior linguistic knowledge influences the
 260 results. Our training uses the standard causal language modeling objective, as in most generative LMs.
 261 To account for variability, we repeat all experiments with 5 random seeds, randomizing both model
 262 initialization and corpus shuffle order. Our primary architecture is Transformer (Vaswani et al., 2017)
 263 in the style of GPT-2 (Radford et al., 2019) with 18, 12, and 4 layers, with all of them having residual
 264

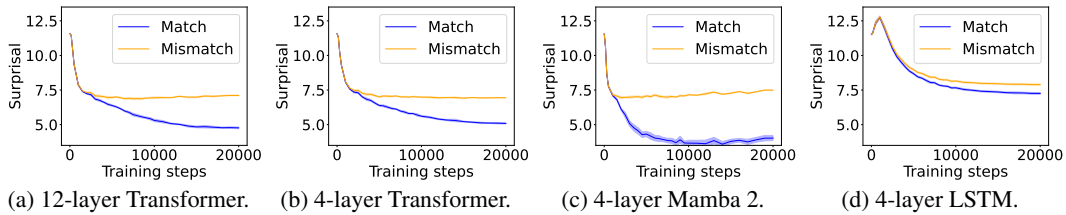


Figure 2: Average surprisal of the experimental and control conditions over training steps.

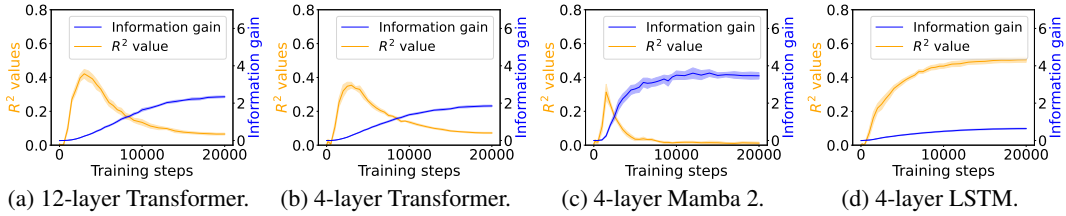


Figure 3: Grounding information gain and its correlation to the co-occurrence of linguistic and environment tokens over training steps.

connections. We extend the experiments to 4-layer unidirectional LSTMs (Hochreiter & Schmidhuber, 1997) with no residual connections, as well as 12- and 4-layer state-space models (specifically, Mamba-2; Dao & Gu, 2024). For fair comparison with LSTMs, the 4-layer Mamba-2 models do not involve residual connections, whereas the 12-layer ones do. For multimodal settings, while standard LLaVA (Liu et al., 2023) uses a two-layer perceptron to project ViT embeddings into the language model, we bypass this projection in our case and directly feed the DINOv2 representations into the LM. We obtain the developmental trajectory of the model by saving checkpoints at various training steps, sampling more heavily from earlier steps, following Chang & Bergen (2022).

4 BEHAVIORAL EVIDENCE

4.1 BEHAVIORAL EVIDENCE OF EMERGENT GROUNDING

In this section, we ask: **Does symbol grounding emerge behaviorally in autoregressive LMs?** We first test whether models show systematic surprisal reduction when predicting a linguistic token when its environmental counterpart is in context (Figure 2, where the gap between the lines represent the grounding information gain). For Transformers (Figures 2a and 2b) and Mamba-2 (Figure 2c), surprisal in the match condition decreases steadily while that in the mismatch condition enters a high-surprisal plateau early, indicating that the models leverage environmental context to predict the linguistic form. In contrast, the unidirectional LSTM (Figure 2d) shows little separation between the conditions, reflecting the absence of grounding. Overall, these results provide behavioral evidence of emergent grounding: in sufficiently expressive architectures (Transformers and Mamba-2), the correct environmental context reliably lowers surprisal for its linguistic counterpart, whereas LSTMs fail to exhibit this effect, marking an architectural boundary on where grounding can emerge.

4.2 BEHAVIORAL EFFECTS BEYOND CO-OCCURRENCE

A natural concern is that the surprisal reductions might be fully explainable by shallow statistics: **the models might have simply memorized frequent co-occurrences of $\langle \text{ENV} \rangle$ and $\langle \text{LAN} \rangle$ tokens, without learning a deeper and more general mapping.** We test this hypothesis by comparing the tokens’ co-occurrence with the grounding information gain in the child-directed speech data.

We define co-occurrence between the corresponding $\langle \text{ENV} \rangle$ and $\langle \text{LAN} \rangle$ tokens at the granularity of a 512-token training chunk. For each target word v , we count the number of chunks in which both its $\langle \text{ENV} \rangle$ and $\langle \text{LAN} \rangle$ tokens appear. Following standard corpus-analysis practice, these raw counts are log-transformed. For each model checkpoint, we run linear regression between the log co-occurrence and the grounding information gain of words, obtaining an R^2 statistic as a function of training time.

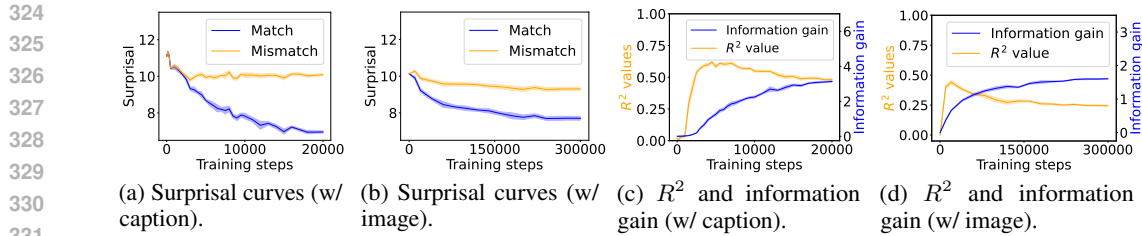


Figure 4: Average surprisal of the experimental and control conditions, as well as the grounding information gain and its correlation to the co-occurrence of linguistic and environment tokens over training steps. All results are from a 12-layer Transformer model on grounded dialogue data.

Figure 3 shows the R^2 values (orange) alongside the grounding information gain (blue) for different architectures. In both the Transformer and Mamba-2, R^2 rises sharply at the early steps but then goes down, even if the grounding information gain continues increasing. These results suggest that grounding in Transformers and Mamba-2 cannot be fully accounted for by co-occurrence statistics: while models initially exploit surface co-occurrence regularities, later improvements in grounding diverge from these statistics, indicating reliance on richer and more complicated features acquired during training. In contrast, LSTM shows persistently increasing R^2 but little increase in grounding information gain over training steps, suggesting that it encodes co-occurrence but lacks the architectural mechanism to transform it into predictive grounding.

4.3 VISUAL DIALOGUE WITH CAPTIONS AND IMAGES

We next test whether the grounding effects observed in CHILDES generalize to multimodal dialogue, using the Visual Dialog dataset. In this setting, the environmental ground is supplied either by captions or by image features (Table 1). For caption-grounded dialogue, the mismatch context is constructed in the same way as for CHILDES (Equation 2). For image-grounded dialogue, mismatch contexts are generated via Stable Diffusion 2 (Rombach et al., 2022)-based image inpainting, which re-generates the region defined by the ground-truth mask corresponding to the target word’s referent.

We train 12-layer Transformers with 5 random seeds. Similarly as Figures 2a–2b and Figures 3a–3b, when captions serve as the environmental ground, Transformers show a clear surprisal gap between match and mismatch conditions (Figure 4a), with the grounding information gain increasing steadily while R^2 peaks early and declines (Figure 4c). Directly using image as grounds yields the same qualitative pattern (Figures 4b and 4d), although the observed effect is smaller. Both settings confirm that emergent grounding cannot be fully explained by co-occurrence statistics.

Overall, our findings demonstrate that Transformers are able to exploit environmental grounds in various modalities to facilitate linguistic prediction. The smaller but consistent gains in the image-grounded case suggest that while grounding from visual tokens is harder, the same architectural dynamics identified in textual testbeds still apply.

5 MECHANISTIC EXPLANATION

In this section, we provide a mechanistic and interpretable account of the previous observation. We first focus on a 12-layer Transformer trained on CHILDES with 5 random seeds, and extend the experiments to image-grounded dialogue (Section 5.4).

5.1 THE EMERGENCE OF SYMBOL GROUNDING

To provide a mechanistic account of symbol grounding, i.e., when it emerges during training and how it is represented in the network, we apply two interpretability analyses.

Saliency flow. For each layer ℓ , we compute a saliency matrix following Wang et al. (2023): $I_\ell = \left| \sum_h A_{h,\ell} \odot \frac{\partial \mathcal{L}}{\partial A_{h,\ell}} \right|$, where $A_{h,\ell}$ denotes the attention matrix of head h in layer ℓ . Each entry of I_ℓ quantifies the contribution of the corresponding attention weight to the cross-entropy loss \mathcal{L} , averaged across heads. Our analysis focuses on ground-to-symbol connections, i.e., flows from environmental ground ($\langle \text{ENV} \rangle$) tokens to the token immediately preceding (and predicting) their linguistic forms ($\langle \text{LAN} \rangle$).

378

379 Probing with the Tuned Lens. We probe layer-wise representations using the Tuned Lens (Belrose et al., 2023), which trains 380 affine projectors to map intermediate activations to the final prediction 381 space while keeping the LM output head frozen.

382

383 Results. Ground-to-symbol saliency is weak in the early stages of 384 training but rises sharply later, peaking in layers 7–9 (Figure 5a), suggesting 385 that mid-layer attention plays a central role in establishing symbol–ground 386 correspondences. In addition, Figure 5b shows that early layers remain poor 387 predictors even at late training stages (e.g., after 20,000 steps), whereas 388 surprisal begins to drop markedly from layer 7 at intermediate stages (step 10,000), 389 suggesting a potential representational shift in the middle layers.

390

391 5.2 HYPOTHESIS: GATHER-AND-AGGREGATE 392 HEADS IMPLEMENT SYMBOL GROUNDING

393

Building on these results, we hypothesize that specific Transformer heads in the middle layers enable symbol grounding. To test this, we examine attention saliencies for selected heads (Figure 6). We find that several heads exhibit patterns consistent with the gather and aggregate mechanisms described by Bick et al. (2025): gather heads (e.g., Figures 6a and 6b) compress relevant information into a subset of positions, while aggregate heads (e.g., Figures 6c and 6d) redistribute this information to downstream tokens. In our setups, saliency often concentrates on environmental tokens such as $\text{train}_{\langle\text{ENV}\rangle}$, where gather heads pool contextual information into compact, retrievable states. In turn, aggregate heads broadcast this information from environmental ground ($\text{train}_{\langle\text{ENV}\rangle}$) to the token immediately preceding the linguistic form, thereby supporting the prediction of $\text{train}_{\langle\text{LAN}\rangle}$. Taking these observations together, we hypothesize that the gather-and-aggregate heads implement the symbol grounding mechanism.

408

409 5.3 CAUSAL INTERVENTIONS OF ATTENTION HEADS 410

411

We then conduct causal interventions of attention heads to validate our previous hypothesis.

412

413 Operational definition. We identify attention heads as gather or aggregate following these standards:

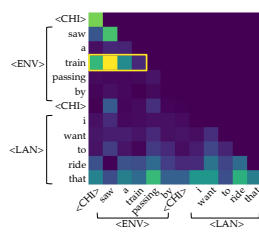
414

- **415 Gather head.** An attention head is classified as a gather head if at least 30% of its total saliency is directed toward the environmental ground token from the previous ones.
- **416 Aggregate head:** An attention head is classified as an aggregate head if at least 30% of its total 417 saliency flows from the environmental ground token to the token immediately preceding the 418 corresponding linguistic token.

419

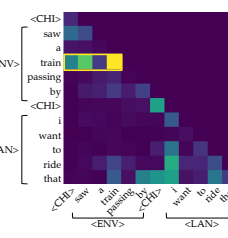
420 Causal intervention methods. In each context, we apply causal interventions to the identified head 421 types and their corresponding controls. Following Bick et al. (2025), interventions are implemented 422 by zeroing out the outputs of heads. For the control, we mask an equal number of randomly selected 423 heads in each layer, ensuring they do not overlap with the identified gather or aggregate heads.

424



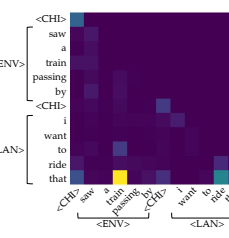
(a) Gather: L4 H7.

425



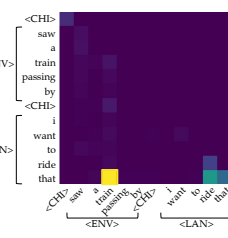
(b) Gather: L4 H8.

426



(c) Aggregate: L7 H5.

427



(d) Aggregate: L8 H5.

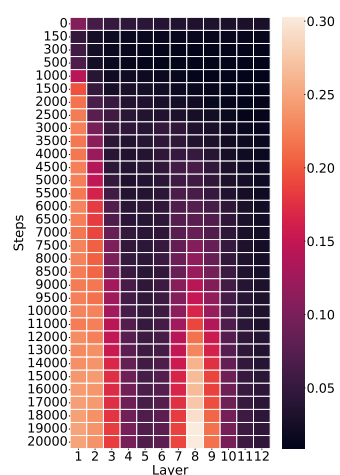
428

429

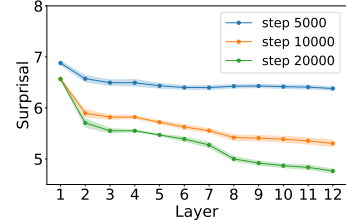
430

431

Figure 6: Examples of gather and aggregate heads identified. L: layer; H: head.



(a) Saliency of layer-wise attention from environmental to linguistic tokens across training steps.



(b) Layer-wise tuned lens to predict the $\langle\text{LAN}\rangle$ token in match condition.

Figure 5: Mechanistic analysis of symbol grounding emergence.

432 **Results and discussions.** As training progresses, the number of both gather and aggregate heads
 433 increases (Table 2), suggesting that these mechanisms emerge over the course of learning. Causal
 434 interventions reveal a clear dissociation: zeroing out aggregate heads consistently produces signif-
 435 icantly higher surprisal compared to controls, whereas the gather head interventions have no such
 436 effect. This asymmetry suggests that gather heads serve in a role less critical in our settings, where
 437 the input template is semantically light and the environmental evidence alone suffices to shape the
 438 linguistic form. Layer-wise patterns further support this division of labor: gather heads cluster in
 439 shallow layers (3-4), while aggregate heads concentrate in mid layers (7-8). This resonates with our
 440 earlier probing results, where surprisal reductions became prominent only from layers 7-9. Together,
 441 these findings highlight aggregate heads in the middle layers as the primary account of grounding in
 442 the model.

443 5.4 GENERALIZATION TO VISUAL DIALOG WITH IMAGES

444 We also conduct causal interventions
 445 of attention heads on the VLM model
 446 to further validate our previous hy-
 447 pothesis.

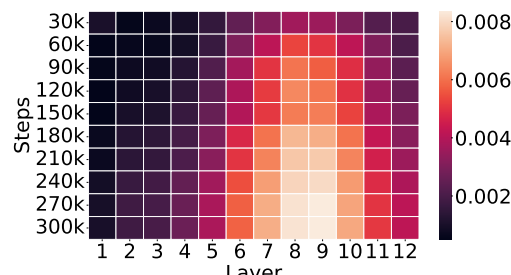
448 **Operational definition.** We identify
 449 attention heads as aggregate following
 450 this standard (We do not define gather
 451 head): An attention head is classified
 452 as an aggregate head if at least a cer-
 453 tain threshold (70% or 90% in our ex-
 454 periment settings) of its total image
 455 patch to end saliency flows from the
 456 patches inside bounding box to the
 457 token immediately preceding the cor-
 458 responding linguistic token.

459 **Causal intervention methods.** In
 460 each context, we apply causal inter-
 461 ventions to the identified head types
 462 and their corresponding controls in the
 463 language backbone of the model. Simi-
 464 lar to section 5.3, interventions are
 465 implemented by zeroing out a head’s
 466 outputs. For the control, we mask an equal number of randomly selected heads in each layer, ensuring
 467 they do not overlap with the identified aggregate heads.

468
 469 Table 2: Causal intervention results on identified gather and
 470 aggregate heads across training checkpoints (ckpt.). **Avg.**
 471 **Count** denotes the average number of heads of each type over
 472 inference times, and **Avg. Layer** denotes the average layer
 473 index where they appear. **Interv. Sps.** reports surprisal after
 474 zeroing out the identified heads, while **Ctrl. Sps.** reports
 475 surprisal after zeroing out an equal number of randomly
 476 selected heads. **Original** refers to the baseline surprisal
 477 without any intervention. *** indicates a significant result
 478 ($p < 0.001$) where the intervention surprisal is higher than
 479 that in the corresponding control experiment.

Ckpt.	Gather Head				Aggregate Head				Original
	Avg. Count	Avg. Layer	Interv. Sps.	Ctrl. Sps.	Avg. Count	Avg. Layer	Interv. Sps.	Ctrl. Sps.	
500	0.00	-	-	-	0.07	8.74	9.34	9.34	9.34
5000	0.35	3.32	6.37	6.38	2.28	7.38	6.51	6.39	6.38
10000	3.26	3.67	5.25	5.32	5.09	7.28	5.86	5.29	5.30
20000	5.76	3.59	4.69	4.79	6.71	7.52	5.62	4.76	4.77

Thres.	Ckpt.	Aggregate Head				Original
		Avg. Count	Avg. Layer	Interv. Sps.	Ctrl. Sps.	
70%	20k	32.30	7.78	9.96	9.95	9.21
	100k	35.63	7.71	9.42 (***)	8.84	8.24
	200k	34.99	7.80	8.95 (***)	8.15	7.76
	300k	34.15	7.76	8.96 (***)	8.11	7.69
	20k	10.66	8.33	9.51 (***)	9.43	9.21
90%	100k	13.90	8.26	8.95 (***)	8.50	8.24
	200k	13.47	8.46	8.41 (***)	7.88	7.76
	300k	12.73	8.42	8.40 (***)	7.87	7.69



481 Figure 7: Mechanistic analysis in the image-grounded visual dialogue setting. Left: Causal inter-
 482 ventions results on identified aggregate heads across training checkpoints, where intervention on aggregate
 483 heads consistently yields significantly higher surprisal ($p < 0.001$, ***) compared to the control group ones.
 484 Right: Saliency of layer-wise attention from environmental tokens (i.e., image tokens
 485 corresponding to patches within the bounding boxes of the target object) to linguistic tokens across
 486 training steps.

486 **Results and discussions.** As training progresses, the number of aggregate heads increases first and
 487 then becomes steady (Figure 7), suggesting that these mechanisms emerge over the course of learning.
 488 Causal interventions reveal that zeroing out aggregate heads consistently produces significantly higher
 489 surprisal rises compared to controls. The average layer also align with the saliency heatmap, also
 490 shown in Figure 7.

491 6 DISCUSSIONS

493 **Generalization to full-scale VLMs.** As an additional case study, we extend our grounding-as-
 494 aggregation hypothesis to a full-scale VLM, LLaVA-1.5-7B (Liu et al., 2023). Even in this heavily
 495 engineered architecture, we identify many attention heads exhibiting aggregation behavior consistent
 496 with our earlier findings (Figure 1b), reinforcing the view that symbol grounding arises from special-
 497 ized heads. At the same time, full-scale VLMs present additional complications. Models like LLaVA
 498 use multiple sets of visual tokens, including CLIP-derived embeddings that already encode language
 499 priors, and global information may be stored in redundant artifact tokens rather than object-centric
 500 regions (Dariset et al., 2024). Moreover, the large number of visual tokens (environmental tokens,
 501 in our setup) substantially increases both computational cost and the difficulty of isolating genuine
 502 aggregation heads. These factors make systematic identification and intervention at scale a nontrivial
 503 challenge. For these reasons, while our case study highlights promising evidence of grounding heads
 504 in modern VLMs, systematic detection and causal evaluation of such heads at scale remains an open
 505 challenge. Future work will need to develop computationally viable methods for (i) automatically
 506 detecting aggregation heads across diverse VLMs, and (ii) applying causal interventions to validate
 507 their role in grounding.

508 **Connection to symbol binding.** While our primary purpose of introducing the minimal testbed
 509 (child-direct speech setting; Table 1) is to offer a proxy for understanding grounding, experiments in
 510 this setting can be naturally viewed as investigations of symbol binding, the problem that studies how
 511 symbols are connected together. This work extends the activation-based study on symbol binding
 512 (Feng & Steinhardt, 2024; Dai et al., 2024; Feng et al., 2025) and offers evidence on the attention-head
 513 level, showing that aggregate heads are crucial in implementing the mechanism (Table 2). In line
 514 with Yang et al. (2025), our work suggests that attention heads are crucial in implementing symbolic
 515 structures in LMs, with more controlled and causal evidence.

516 **The philosophical roots of grounding, revisited.** Our findings highlight the need to sharpen
 517 the meaning of grounding in multimodal models. Prior work has often equated grounding with
 518 statistical correlations between visual and textual signals, such as attention overlaps or geometric
 519 alignments (Cao et al., 2024; Bousselham et al., 2024; Schnaus et al., 2025). While informative,
 520 such correlations diverge from the classic formulation by Harnad (1990), which requires symbols
 521 to be causally anchored to their referents in the environment. In line with Harnad (1990), we
 522 frame grounding as a mechanistic property: one that can be traced along training, observed in the
 523 specialization of attention heads, and validated through causal interventions, providing a protocol for
 524 diagnosing when and how models genuinely tie symbols to meaning rather than mere correlations.
 525 **On another line, our results, which show that aggregate heads implement symbol grounding (and**
 526 **binding), echo Pavlick (2023) in arguing that LLMs lack the capacity to represent abstract symbolic**
 527 **structure** should not be accepted a priori. Instead, such claims should be evaluated carefully and
 528 empirically, with the focus on uncovering the models’ underlying competence rather than drawing
 529 conclusions solely from high-level architectures and surface-level performance.

530 **Practical implications to LM hallucinations.** Our findings have practical implications for improving
 531 the reliability of LM outputs: by identifying aggregation heads that mediate grounding between
 532 environmental and linguistic tokens, we provide a promising mechanism to detect model reliability
 533 before generation. Our findings echo a pathway to mitigate hallucinations by focusing on attention
 534 control: many hallucination errors stem from misallocated attention in intermediate layers (Jiang et al.,
 535 2025; Chen et al., 2024b). Such attention-level signals can serve as early indicators of overtrust or
 536 false grounding, motivating practical solutions like decoding-time strategies to mitigate and eventually
 537 prevent hallucination (Huang et al., 2024).

538
 539

540
541 ETHICS STATEMENT542
543 This study analyzes the mechanistic emergence of symbol grounding in language models using
544 publicly available datasets such as CHILDES and Visual Dialog. All the images are from the publicly
545 available MSCOCO dataset (Lin et al., 2014) where no personally identifiable data is used.546
547 REPRODUCIBILITY STATEMENT548
549 We describe dataset construction, tokenization schemes, evaluation protocols, and model training
550 settings in detail within the main text and Appendix. All experiments were repeated with multiple
551 random seeds, and results across different architectures are reported. Code and data processing
552 scripts are included in supplementary materials and will be released upon acceptance to facilitate full
553 reproducibility.554
555 REFERENCES556
557 Anthropic. The claude 3 model family: Opus, sonnet, haiku, March 2024. URL <https://www.anthropic.com/news/clause-3-family>.558
559 Aryaman Arora, Neil Rathi, Nikil Roashan Selvam, Róbert Csórdas, Dan Jurafsky, and Christo-
560 pher Potts. Mechanistic evaluation of transformers and state space models. *arXiv preprint*
561 *arXiv:2505.15105*, 2025.562
563 Nora Belrose, Zach Furman, Logan Smith, Danny Halawi, Igor Ostrovsky, Lev McKinney, Stella
564 Biderman, and Jacob Steinhardt. Eliciting latent predictions from transformers with the tuned lens.
565 *arXiv preprint arXiv:2303.08112*, 2023.566
567 Aviv Bick, Eric P. Xing, and Albert Gu. Understanding the skill gap in recurrent models: The role
568 of the gather-and-aggregate mechanism. In *Forty-second International Conference on Machine
Learning*, 2025.569
570 Stella Biderman, Hailey Schoelkopf, Quentin Gregory Anthony, Herbie Bradley, Kyle O'Brien, Eric
571 Hallahan, Mohammad Aftab Khan, Shivanshu Purohit, USVSN Sai Prashanth, Edward Raff, et al.
572 Pythia: A suite for analyzing large language models across training and scaling. In *International
Conference on Machine Learning*, pp. 2397–2430. PMLR, 2023.573
574 Alberto Bietti, Vivien Cabannes, Diane Bouchacourt, Hervé Jegou, and Leon Bottou. Birth of a
575 transformer: A memory viewpoint. *arXiv preprint arXiv:2306.00802*, 2023.576
577 Terra Blevins, Hila Gonen, and Luke Zettlemoyer. Analyzing the mono-and cross-lingual pretraining
578 dynamics of multilingual language models. In *Proceedings of the 2022 Conference on Empirical
Methods in Natural Language Processing*, pp. 3575–3590, 2022.579
580 Walid Bousselham, Felix Petersen, Vittorio Ferrari, and Hilde Kuehne. Grounding everything:
581 Emerging localization properties in vision-language transformers. In *Proceedings of the IEEE/CVF
Conference on Computer Vision and Pattern Recognition*, pp. 3828–3837, 2024.583
584 Shengcao Cao, Liang-Yan Gui, and Yu-Xiong Wang. Emerging pixel grounding in large multimodal
585 models without grounding supervision. *arXiv preprint arXiv:2410.08209*, 2024.586
587 Tyler A Chang and Benjamin K Bergen. Word acquisition in neural language models. *Transactions
of the Association for Computational Linguistics*, 10:1–16, 2022.588
589 Tyler A Chang, Zhuowen Tu, and Benjamin K Bergen. Characterizing learning curves during
590 language model pre-training: Learning, forgetting, and stability. *Transactions of the Association
591 for Computational Linguistics*, 12:1346–1362, 2024.592
593 Jierun Chen, Fangyun Wei, Jinjing Zhao, Sizhe Song, Bohuai Wu, Zhuoxuan Peng, S-H Gary Chan,
594 and Hongyang Zhang. Revisiting referring expression comprehension evaluation in the era of large
595 multimodal models. *arXiv preprint arXiv:2406.16866*, 2024a.

594 Keqin Chen, Zhao Zhang, Weili Zeng, Richong Zhang, Feng Zhu, and Rui Zhao. Shikra: Unleashing
 595 multimodal llm's referential dialogue magic. *arXiv preprint arXiv:2306.15195*, 2023.
 596

597 Xuweiyi Chen, Ziqiao Ma, Xuejun Zhang, Sihan Xu, Shengyi Qian, Jianing Yang, David Fouhey, and
 598 Joyce Chai. Multi-object hallucination in vision language models. *Advances in Neural Information
 599 Processing Systems*, 37:44393–44418, 2024b.

600 Eve V Clark. *The lexicon in acquisition*. Number 65. Cambridge University Press, 1995.
 601

602 Gheorghe Comanici, Eric Bieber, Mike Schaeckermann, Ice Pasupat, Noveen Sachdeva, Inderjit
 603 Dhillon, Marcel Blistein, Ori Ram, Dan Zhang, Evan Rosen, et al. Gemini 2.5: Pushing the frontier
 604 with advanced reasoning, multimodality, long context, and next generation agentic capabilities.
 605 *arXiv preprint arXiv:2507.06261*, 2025.

606 Qin Dai, Benjamin Heinzerling, and Kentaro Inui. Representational analysis of binding in language
 607 models. In Yaser Al-Onaizan, Mohit Bansal, and Yun-Nung Chen (eds.), *Proceedings of the
 608 2024 Conference on Empirical Methods in Natural Language Processing*, pp. 17468–17493,
 609 Miami, Florida, USA, November 2024. Association for Computational Linguistics. URL <https://aclanthology.org/2024.emnlp-main.967/>.
 610

611 Tri Dao and Albert Gu. Transformers are ssms: Generalized models and efficient algorithms through
 612 structured state space duality. In *International Conference on Machine Learning*, pp. 10041–10071.
 613 PMLR, 2024.

614 Timothée Darcet, Maxime Oquab, Julien Mairal, and Piotr Bojanowski. Vision transformers need
 615 registers. In *The Twelfth International Conference on Learning Representations*, 2024.

616 Abhishek Das, Satwik Kottur, Khushi Gupta, Avi Singh, Deshraj Yadav, José MF Moura, Devi Parikh,
 617 and Dhruv Batra. Visual dialog. In *Proceedings of the IEEE conference on computer vision and
 618 pattern recognition*, pp. 326–335, 2017.

619 Alexey Dosovitskiy, Lucas Beyer, Alexander Kolesnikov, Dirk Weissenborn, Xiaohua Zhai, Thomas
 620 Unterthiner, Mostafa Dehghani, Matthias Minderer, Georg Heigold, Sylvain Gelly, et al. An image
 621 is worth 16x16 words: Transformers for image recognition at scale. In *International Conference
 622 on Learning Representations*, 2020.

623 Nelson Elhage, Neel Nanda, Catherine Olsson, Tom Henighan, Nicholas Joseph, Ben Mann, Amanda
 624 Askell, Yuntao Bai, Anna Chen, Tom Conerly, Nova DasSarma, Dawn Drain, Deep Ganguli,
 625 Zac Hatfield-Dodds, Danny Hernandez, Andy Jones, Jackson Kernion, Liane Lovitt, Kamal
 626 Ndousse, Dario Amodei, Tom Brown, Jack Clark, Jared Kaplan, Sam McCandlish, and Chris
 627 Olah. A mathematical framework for transformer circuits. *Transformer Circuits Thread*, 2021.
 628 <https://transformer-circuits.pub/2021/framework/index.html>.
 629

630 Linnea Evanson, Yair Lakretz, and Jean-Rémi King. Language acquisition: do children and lan-
 631 guage models follow similar learning stages? In *Findings of the Association for Computational
 632 Linguistics: ACL 2023*, pp. 12205–12218, 2023.

633 Afsaneh Fazly, Afra Alishahi, and Suzanne Stevenson. A probabilistic computational model of
 634 cross-situational word learning. *Cognitive Science*, 34(6):1017–1063, 2010.

635 Jiahai Feng and Jacob Steinhardt. How do language models bind entities in context? In *The Twelfth
 636 International Conference on Learning Representations*, 2024. URL [https://openreview.net/
 637 forum?id=zb3b60K077](https://openreview.net/forum?id=zb3b60K077).

638 Jiahai Feng, Stuart Russell, and Jacob Steinhardt. Monitoring latent world states in language models
 639 with propositional probes. In *The Thirteenth International Conference on Learning Representations*,
 640 2025. URL <https://openreview.net/forum?id=0yvZm2AjUr>.

641 Larry Fenson, Virginia A Marchman, Donna J Thal, Phillip S Dale, J Steven Reznick, and Elizabeth
 642 Bates. Macarthur-bates communicative development inventories. *PsycTESTS Dataset*, 2006.
 643

644 Lila R Gleitman and Barbara Landau. *The acquisition of the lexicon*. mit Press, 1994.

648 Noah Goodman, Joshua Tenenbaum, and Michael Black. A bayesian framework for cross-situational
 649 word-learning. *Advances in neural information processing systems*, 20, 2007.
 650

651 Thilo Hagendorff. Machine psychology: Investigating emergent capabilities and behavior in large
 652 language models using psychological methods. *arXiv preprint arXiv:2303.13988*, 2023.
 653

654 Stevan Harnad. The symbol grounding problem. *Physica D: Nonlinear Phenomena*, 42(1-3):335–346,
 655 1990.
 656

657 Sepp Hochreiter and Jürgen Schmidhuber. Long short-term memory. *Neural computation*, 9(8):
 658 1735–1780, 1997.
 659

660 Qidong Huang, Xiaoyi Dong, Pan Zhang, Bin Wang, Conghui He, Jiaqi Wang, Dahua Lin, Weiming
 661 Zhang, and Nenghai Yu. Opera: Alleviating hallucination in multi-modal large language models
 662 via over-trust penalty and retrospection-allocation. In *Proceedings of the IEEE/CVF Conference
 663 on Computer Vision and Pattern Recognition*, pp. 13418–13427, 2024.
 664

665 Zhangqi Jiang, Junkai Chen, Beier Zhu, Tingjin Luo, Yankun Shen, and Xu Yang. Devils in middle
 666 layers of large vision-language models: Interpreting, detecting and mitigating object hallucinations
 667 via attention lens. In *Proceedings of the Computer Vision and Pattern Recognition Conference*, pp.
 668 25004–25014, 2025.
 669

670 Sara Kangaslahti, Elan Rosenfeld, and Naomi Saphra. Hidden breakthroughs in language model
 671 training. *arXiv preprint arXiv:2506.15872*, 2025.
 672

673 Liunian Harold Li, Pengchuan Zhang, Haotian Zhang, Jianwei Yang, Chunyuan Li, Yiwu Zhong,
 674 Lijuan Wang, Lu Yuan, Lei Zhang, Jenq-Neng Hwang, et al. Grounded language-image pre-training.
 675 In *Proceedings of the IEEE/CVF Conference on Computer Vision and Pattern Recognition*, pp.
 676 10965–10975, 2022.
 677

678 Tom Lieberum, Matthew Rahtz, János Kramár, Neel Nanda, Geoffrey Irving, Rohin Shah, and
 679 Vladimir Mikulik. Does circuit analysis interpretability scale? evidence from multiple choice
 680 capabilities in chinchilla. *arXiv preprint arXiv:2307.09458*, 2023.
 681

682 Tsung-Yi Lin, Michael Maire, Serge Belongie, James Hays, Pietro Perona, Deva Ramanan, Piotr
 683 Dollár, and C Lawrence Zitnick. Microsoft coco: Common objects in context. In *European
 684 conference on computer vision*, pp. 740–755. Springer, 2014.
 685

686 Haotian Liu, Chunyuan Li, Qingyang Wu, and Yong Jae Lee. Visual instruction tuning. In *Advances
 687 in neural information processing systems*, volume 36, pp. 34892–34916, 2023.
 688

689 Sheng Lu, Irina Bigoulaeva, Rachneet Sachdeva, Harish Tayyar Madabushi, and Iryna Gurevych.
 690 Are emergent abilities in large language models just in-context learning? *arXiv preprint
 691 arXiv:2309.01809*, 2023.
 692

693 Ziqiao Ma, Jiayi Pan, and Joyce Chai. World-to-words: Grounded open vocabulary acquisition
 694 through fast mapping in vision-language models. In *Proceedings of the 61st Annual Meeting of the
 695 Association for Computational Linguistics (Volume 1: Long Papers)*, pp. 524–544, 2023.
 696

697 Ziqiao Ma, Zekun Wang, and Joyce Chai. Babysit a language model from scratch: Interactive
 698 language learning by trials and demonstrations. In *Proceedings of the 2025 Conference of the
 699 Nations of the Americas Chapter of the Association for Computational Linguistics: Human
 700 Language Technologies (Volume 1: Long Papers)*, pp. 991–1010, 2025.
 701

702 Brian MacWhinney. The childe project: Tools for analyzing talk: Volume i: Transcription format
 703 and programs, volume ii: The database, 2000.
 704

705 Jiayuan Mao, Chuang Gan, Pushmeet Kohli, Joshua B. Tenenbaum, and Jiajun Wu. The neuro-
 706 symbolic concept learner: Interpreting scenes, words, sentences from natural supervision. *Inter-
 707 national Conference on Learning Representations (ICLR)*, 2019.
 708

709 Jiayuan Mao, Freda H. Shi, Jiajun Wu, Roger P. Levy, and Joshua B. Tenenbaum. Grammar-based
 710 grounded lexicon learning. In A. Beygelzimer, Y. Dauphin, P. Liang, and J. Wortman Vaughan
 711 (eds.), *Advances in Neural Information Processing Systems*, 2021.

702 Kevin Meng, David Bau, Alex Andonian, and Yonatan Belinkov. Locating and editing factual
 703 associations in gpt. *arXiv preprint arXiv:2202.05262*, 2023.

704 Catherine Olsson, Nelson Elhage, Neel Nanda, Nicholas Joseph, Nova DasSarma, Tom Henighan,
 705 Ben Mann, Amanda Askell, Yuntao Bai, Anna Chen, Tom Conerly, Dawn Drain, Deep Ganguli,
 706 Zac Hatfield-Dodds, Danny Hernandez, Scott Johnston, Andy Jones, Jackson Kernion, Liane
 707 Lovitt, Kamal Ndousse, Dario Amodei, Tom Brown, Jack Clark, Jared Kaplan, Sam McCandlish,
 708 and Chris Olah. In-context learning and induction heads. *Transformer Circuits Thread*, 2022.
 709 <https://transformer-circuits.pub/2022/in-context-learning-and-induction-heads/index.html>.

710

711 OpenAI. Hello gpt-4o, May 2024. URL <https://openai.com/index/hello-gpt-4o/>.

712 Maxime Oquab, Timothée Darcet, Théo Moutakanni, Huy Vo, Marc Szafraniec, Vasil Khalidov,
 713 Pierre Fernandez, Daniel Haziza, Francisco Massa, Alaaeldin El-Nouby, et al. Dinov2: Learning
 714 robust visual features without supervision. *Transactions on Machine Learning Research Journal*,
 715 pp. 1–31, 2024.

716

717 Ellie Pavlick. Symbols and grounding in large language models. *Philosophical Transactions of the
 718 Royal Society A: Mathematical, Physical and Engineering Sciences*, 381(2251):20220041, 2023.
 719 doi: 10.1098/rsta.2022.0041.

720 Zhiliang Peng, Wenhui Wang, Li Dong, Yaru Hao, Shaohan Huang, Shuming Ma, Qixiang Ye, and
 721 Furu Wei. Grounding multimodal large language models to the world. In *The Twelfth International
 722 Conference on Learning Representations*, 2024.

723 Sarah Pratt, Mark Yatskar, Luca Weihs, Ali Farhadi, and Aniruddha Kembhavi. Grounded situation
 724 recognition. In *European Conference on Computer Vision*, pp. 314–332. Springer, 2020.

725

726 Shaolin Qu and Joyce Yue Chai. Context-based word acquisition for situated dialogue in a virtual
 727 world. *Journal of Artificial Intelligence Research*, 37:247–277, 2010.

728

729 Alec Radford, Jeffrey Wu, Rewon Child, David Luan, Dario Amodei, Ilya Sutskever, et al. Language
 730 models are unsupervised multitask learners. *OpenAI blog*, 1(8):9, 2019.

731 Alec Radford, Jong Wook Kim, Chris Hallacy, Aditya Ramesh, Gabriel Goh, Sandhini Agarwal,
 732 Girish Sastry, Amanda Askell, Pamela Mishkin, Jack Clark, et al. Learning transferable visual
 733 models from natural language supervision. In *International conference on machine learning*, pp.
 734 8748–8763. PMLR, 2021.

735 Hanoona Rasheed, Muhammad Maaz, Sahal Shaji, Abdelrahman Shaker, Salman Khan, Hisham
 736 Cholakkal, Rao M Anwer, Erix Xing, Ming-Hsuan Yang, and Fahad S Khan. Glamm: Pixel
 737 grounding large multimodal model. In *Proceedings of the IEEE/CVF Conference on Computer
 738 Vision and Pattern Recognition*, 2024.

739

740 Terry Regier. The emergence of words: Attentional learning in form and meaning. *Cognitive science*,
 741 29(6):819–865, 2005.

742 Robin Rombach, Andreas Blattmann, Dominik Lorenz, Patrick Esser, and Björn Ommer. High-
 743 resolution image synthesis with latent diffusion models. In *Proceedings of the IEEE/CVF confer-
 744 ence on computer vision and pattern recognition*, pp. 10684–10695, 2022.

745

746 Deb K Roy and Alex P Pentland. Learning words from sights and sounds: A computational model.
 747 *Cognitive science*, 26(1):113–146, 2002.

748

749 Masoud Jalili Sabet, Philipp Dufter, François Yvon, and Hinrich Schütze. Simalign: High quality
 750 word alignments without parallel training data using static and contextualized embeddings. In
 751 *Findings of the Association for Computational Linguistics: EMNLP 2020*, 2020.

752

753 Rylan Schaeffer, Brando Miranda, and Sanmi Koyejo. Are emergent abilities of large language
 754 models a mirage? *Advances in Neural Information Processing Systems*, 36, 2023.

755 Dominik Schnaus, Nikita Araslanov, and Daniel Cremers. It’s a (blind) match! towards vision-
 756 language correspondence without parallel data. In *Proceedings of the Computer Vision and Pattern
 757 Recognition Conference*, pp. 24983–24992, 2025.

756 Thibault Sellam, Steve Yadlowsky, Ian Tenney, Jason Wei, Naomi Saphra, Alexander D’Amour,
 757 Tal Linzen, Jasmijn Bastings, Iulia Raluca Turc, Jacob Eisenstein, et al. The multiberts: Bert
 758 reproductions for robustness analysis. In *International Conference on Learning Representations*,
 759 2021.

760 Haoyue Shi, Luke Zettlemoyer, and Sida I. Wang. Bilingual lexicon induction via unsupervised
 761 bitext construction and word alignment. In *ACL*, 2021. URL <https://aclanthology.org/2021.acl-long.67/>.

762

763 Jeffrey Mark Siskind. A computational study of cross-situational techniques for learning word-to-
 764 meaning mappings. *Cognition*, 61(1-2):39–91, 1996.

765

766 Oskar van der Wal, Pietro Lesci, Max Müller-Eberstein, Naomi Saphra, Hailey Schoelkopf, Willem
 767 Zuidema, and Stella Biderman. Polypythias: Stability and outliers across fifty language model
 768 pre-training runs. In *Proceedings of the Thirteenth International Conference on Learning Repre-
 769 sentations (ICLR 2025)*, pp. 1–25, 2025.

770

771 Ashish Vaswani, Noam Shazeer, Niki Parmar, Jakob Uszkoreit, Llion Jones, Aidan N Gomez, Łukasz
 772 Kaiser, and Illia Polosukhin. Attention is all you need. *Advances in neural information processing
 773 systems*, 30, 2017.

774

775 Lean Wang, Lei Li, Damai Dai, Deli Chen, Hao Zhou, Fandong Meng, Jie Zhou, and Xu Sun. Label
 776 words are anchors: An information flow perspective for understanding in-context learning. In
 777 *Proceedings of the 2023 Conference on Empirical Methods in Natural Language Processing*, pp.
 778 9840–9855, 2023.

779

780 Weihuan Wang, Qingsong Lv, Wenmeng Yu, Wenyi Hong, Ji Qi, Yan Wang, Junhui Ji, Zhuoyi Yang,
 781 Lei Zhao, Song XiXuan, et al. Cogvlm: Visual expert for pretrained language models. *Advances
 782 in Neural Information Processing Systems*, 37:121475–121499, 2024.

783

784 Jason Wei, Yi Tay, Rishi Bommasani, Colin Raffel, Barret Zoph, Sebastian Borgeaud, Dani Yogatama,
 785 Maarten Bosma, Denny Zhou, Donald Metzler, et al. Emergent abilities of large language models.
 786 *Transactions on Machine Learning Research*, 2022.

787

788 Sarah Wiegreffe, Oyvind Tafjord, Yonatan Belinkov, Hannaneh Hajishirzi, and Ashish Sabharwal.
 789 Answer, assemble, ace: Understanding how lms answer multiple choice questions. *arXiv preprint
 790 arXiv:2407.15018*, 2025.

791

792 Wenhao Wu, Yizhong Wang, Guangxuan Xiao, Hao Peng, and Yao Fu. Retrieval head mechanistically
 793 explains long-context factuality. *arXiv preprint arXiv:2404.15574*, 2024.

794

795 Zhaofeng Wu, Dani Yogatama, Jiasen Lu, and Yoon Kim. The semantic hub hypothesis: Language
 796 models share semantic representations across languages and modalities. In *ICML*, 2025.

797

798 Mengzhou Xia, Mikel Artetxe, Chunting Zhou, Xi Victoria Lin, Ramakanth Pasunuru, Danqi Chen,
 799 Luke Zettlemoyer, and Ves Stoyanov. Training trajectories of language models across scales. In
 800 *Proceedings of the 61st Annual Meeting of the Association for Computational Linguistics (Volume
 1: Long Papers)*, pp. 13711–13738, 2023.

801

802 Zhuofan Xia, Dongchen Han, Yizeng Han, Xuran Pan, Shiji Song, and Gao Huang. Gsва: Generalized
 803 segmentation via multimodal large language models. In *Proceedings of the IEEE/CVF Conference
 804 on Computer Vision and Pattern Recognition*, 2024.

805

806 Fei Xu and Joshua B Tenenbaum. Word learning as bayesian inference. *Psychological review*, 114
 807 (2):245, 2007.

808

809 Yukang Yang, Declan Iain Campbell, Kaixuan Huang, Mengdi Wang, Jonathan D. Cohen, and
 810 Taylor Whittington Webb. Emergent symbolic mechanisms support abstract reasoning in large
 811 language models. In *Forty-second International Conference on Machine Learning*, 2025. URL
 812 <https://openreview.net/forum?id=y1SnRPDWx4>.

813

814 Haoxuan You, Haotian Zhang, Zhe Gan, Xianzhi Du, Bowen Zhang, Zirui Wang, Liangliang Cao,
 815 Shih-Fu Chang, and Yinfei Yang. Ferret: Refer and ground anything anywhere at any granularity.
 816 In *The Twelfth International Conference on Learning Representations*, 2024.

810 Chen Yu. The emergence of links between lexical acquisition and object categorization: A computational
811 study. *Connection science*, 17(3-4):381–397, 2005.

812
813 Chen Yu and Dana H Ballard. A unified model of early word learning: Integrating statistical and
814 social cues. *Neurocomputing*, 70(13-15):2149–2165, 2007.

815 Haonan Yu and Jeffrey Mark Siskind. Grounded language learning from video described with
816 sentences. In *Proceedings of the 51st Annual Meeting of the Association for Computational
817 Linguistics (Volume 1: Long Papers)*, pp. 53–63, 2013.

818 Tao Zhang, Xiangtai Li, Hao Fei, Haobo Yuan, Shengqiong Wu, Shunping Ji, Chen Change Loy,
819 and Shuicheng Yan. Omg-llava: Bridging image-level, object-level, pixel-level reasoning and
820 understanding. *Advances in neural information processing systems*, 37:71737–71767, 2024a.

821 Yichi Zhang, Ziqiao Ma, Xiaofeng Gao, Suhaila Shakiah, Qiaozi Gao, and Joyce Chai. Groundhog:
822 Grounding large language models to holistic segmentation. In *Proceedings of the IEEE/CVF
823 Conference on Computer Vision and Pattern Recognition*, 2024b.

824
825 Rosie Zhao, Tian Qin, David Alvarez-Melis, Sham Kakade, and Naomi Saphra. Distributional scaling
826 laws for emergent capabilities. *arXiv preprint arXiv:2502.17356*, 2025.

827
828
829
830
831
832
833
834
835
836
837
838
839
840
841
842
843
844
845
846
847
848
849
850
851
852
853
854
855
856
857
858
859
860
861
862
863

864 **A DATASET DETAILS**

865

866 **A.1 CONTEXT TEMPLATES**

867

868 We select the target tokens following the given procedure:

869

1. Get a list of words, with their ENV and LAN frequency both greater than or equal to 100 in the CHILDES dataset;
2. Get another list of nouns from CDI;
3. Take intersection and select top 100 words (by frequency of their ENV token) as target token list.

870 In CHILDES, all contexts are created with gpt-4o-mini followed by human verification if the
 871 generated contexts are semantically light. We adopt the following prompt:
 872

873

874

875

876

877

878

Prompt Templates for CHILDES

879 Given the word “{word}”, create 3 pairs of sentences that follow this
 880 requirement:
 881 1. The first sentence has a subject “The child”, describing an event or
 882 situation, and has the word “{word}”. Make sure to add a newline to the end of
 883 this first sentence
 884 2. The second sentence is said by the child (only include the speech itself,
 885 don't include “the child say”, etc.), and the word “{word}” also appears in
 886 the sentence said by the child. Do not add quote marks either
 887 3. Print each sentence on one line. Do not include anything else.
 888 4. Each sentence should be short, less than 10 words.
 889 5. The word “{word}” in both sentence have the same meaning and have a clear
 890 indication or an implication relationship.
 891 6. “{word}” should not appear at the first/second word of each sentence.
 892 Generate 3 pairs of such sentences, so there should be 6 lines in total.
 893 You should not add a number.
 894 For each line, just print out the sentence.

895

896

In visual dialogue (caption version and VLM version), we pre-define 10 sets of templates for each
 897 version:

898

899

Prompt Templates for Visual Dialogue (Caption Version)

900 this:<ENV> is:<ENV> [FILLER]:<ENV> <Q> what:<LAN> is:<LAN> it:<LAN> <A>
 901 (predict [FILLER]:<LAN>)
 902
 903 this:<ENV> is:<ENV> [FILLER]:<ENV> <Q> what:<LAN> do:<LAN> you:<LAN>
 904 call:<LAN> this:<LAN> <A> (predict [FILLER]:<LAN>)
 905
 906 this:<ENV> is:<ENV> [FILLER]:<ENV> <Q> can:<LAN> you:<LAN>
 907 name:<LAN> this:<LAN> object:<LAN> <A>
 908 (predict [FILLER]:<LAN>)
 909
 910 this:<ENV> is:<ENV> [FILLER]:<ENV> <Q> what's:<LAN>
 911 this:<LAN> called:<LAN> <A>
 912 (predict [FILLER]:<LAN>)
 913
 914 this:<ENV> is:<ENV> [FILLER]:<ENV> <Q> what:<LAN>
 915 this:<LAN> thing:<LAN> is:<LAN> <A>
 916 (predict [FILLER]:<LAN>)

917

918
919

Prompt Templates for Visual Dialogue (Caption Version) (continued)

```

920 this:<ENV> is:<ENV> [FILLER]:<ENV> <Q> what:<LAN>
921 would:<LAN> you:<LAN> name:<LAN> this:<LAN> <A>
922 (predict [FILLER]:<LAN>)

923 this:<ENV> is:<ENV> [FILLER]:<ENV> <Q>
924 what's:<LAN> the:<LAN> name:<LAN> of:<LAN> this:<LAN>
925 item:<LAN> <A> (predict [FILLER]:<LAN>)

927 this:<ENV> is:<ENV> [FILLER]:<ENV> <Q> how:<LAN>
928 do:<LAN> you:<LAN> identify:<LAN> this:<LAN> <A>
929 (predict [FILLER]:<LAN>)

931 this:<ENV> is:<ENV> [FILLER]:<ENV> <Q> what:<LAN>
932 do:<LAN> we:<LAN> have:<LAN> here:<LAN> <A>
933 (predict [FILLER]:<LAN>)

934 this:<ENV> is:<ENV> [FILLER]:<ENV> <Q> how:<LAN>
935 do:<LAN> you:<LAN> call:<LAN> this:<LAN>
936 object:<LAN> <A> (predict [FILLER]:<LAN>)

938
939
940

```

941
942

Prompt Templates for Visual Dialogue (VLM Version)

```

943 "<image> \nwhat is it ?",
944 "<image> \nwhat do you call this ?",
945 "<image> \ncan you name this object ?",
946 "<image> \nwhat is this called ?",
947 "<image> \nwhat this thing is ?",
948 "<image> \nwhat would you name this ?",
949 "<image> \nwhat is the name of this item ?",
950 "<image> \nhow do you identify this ?",
951 "<image> \nwhat do we have here ?",
952 "<image> \nhow do you call this object ?"

953
954

```

955
956

A.2 WORD LIST FOR CHILDES AND VISION DIALOGUE (TEXT ONLY)

957
958
959
960
961
962
963
964

[box, book, ball, hand, paper, table, toy, head, car, chair, room, picture, doll, cup, towel, door, mouth, camera, duck, face, truck, bottle, puzzle, bird, tape, finger, bucket, block, stick, elephant, hat, bed, arm, dog, kitchen, spoon, hair, blanket, horse, tray, train, cow, foot, couch, necklace, cookie, plate, telephone, window, brush, ear, pig, purse, hammer, cat, shoulder, garage, button, monkey, pencil, shoe, drawer, leg, bear, milk, egg, bowl, juice, ladder, basket, coffee, bus, food, apple, bench, sheep, airplane, comb, bread, eye, animal, knee, shirt, cracker, glass, light, game, cheese, sofa, giraffe, turtle, stove, clock, star, refrigerator, banana, napkin, bunny, farm, money]

965
966

A.3 WORD LIST FOR VISION DIALOGUE (VLM)

967
968
969
970
971

[box, book, table, toy, car, chair, doll, door, camera, duck, truck, bottle, bird, elephant, hat, bed, dog, spoon, horse, train, couch, necklace, cookie, plate, telephone, window, pig, cat, monkey, drawer, bear, milk, egg, bowl, juice, ladder, bus, food, apple, sheep, bread, animal, shirt, cheese, giraffe, clock, refrigerator, accordion, aircraft, alpaca, ambulance, ant, antelope, backpack, bagel, balloon, barrel, bathtub, beard, bee, beer, beetle, bicycle, bidet, billboard, boat, bookcase, boot, boy, broccoli, building, bull, burrito, bust, butterfly, cabbage, cabinetry, cake, camel, canary, candle, candy, cannon,

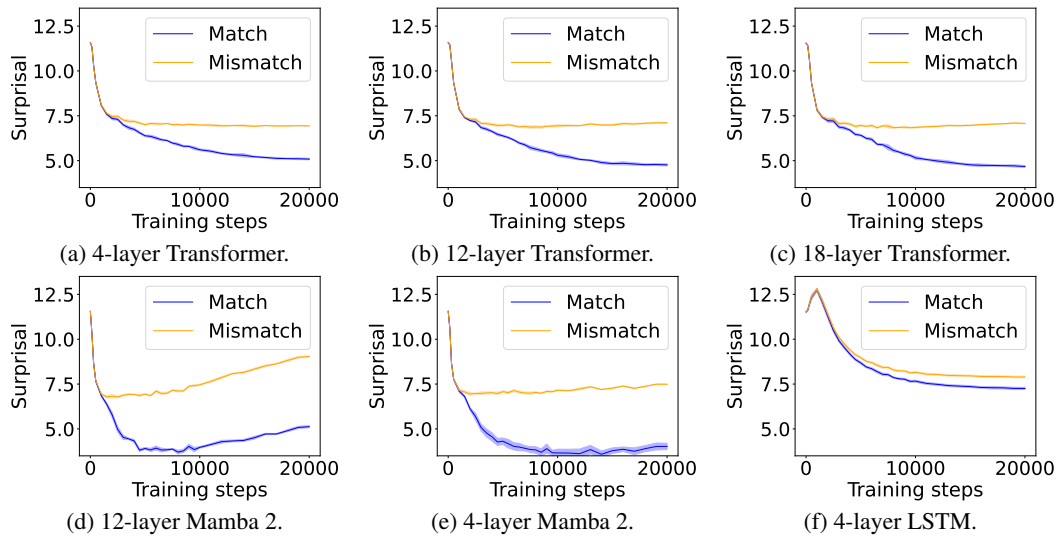


Figure 8: Average surprisal of the experimental and control conditions over training steps.

canoe, carrot, cart, castle, caterpillar, cattle, cello, cheetah, chicken, chopsticks, closet, clothing, coat, cocktail, coffeemaker, coin, cosmetics]

B IMPLEMENTATION DETAILS

B.1 CHECKPOINTING

B.1.1 CHILDES, VISUAL DIALOGUE WITH CAPTIONS

We save the intermediate steps: [0, 150, 300, 500, 1000, 1500, 2000, 2500, 3000, 3500, 4000, 4500, 5000, 5500, 6000, 6500, 7000, 7500, 8000, 8500, 9000, 9500, 10000, 11000, 12000, 13000, 14000, 15000, 16000, 17000, 18000, 19000, 20000] (33 checkpoints in total)

B.1.2 VISUAL DIALOGUE (VLM)

We save the intermediate steps: [10000, 20000, 40000, 60000, 80000, 100000, 120000, 140000, 160000, 180000, 200000, 220000, 240000, 260000, 280000, 300000] (16 checkpoints in total)

C ADDENDUM TO RESULTS

C.1 DETAILED BEHAVIORAL ANALYSIS FOR ALL MODELS

We show the complete behavioral evidence for all models in Figure 8, and co-occurrence analysis in Figure 9. **On top of that, a beeswarm plot indicating per context match/mismatch surprisal is shown in Figure 10.**

C.2 DETAILED GATHER AND AGGREGATE ANALYSIS (TRANSFORMER)

After finding the set of gather and aggregate heads for each context, we run an overtime analysis showing the proportion of saliency to the total saliency, as is shown in Figure 11.

C.3 RELATIONSHIP BETWEEN AGGREGATE HEAD NUMBER AND GROUNDING INFORMATION GAIN

We examine the 12-layer Transformer LM for both the child-directed speech and VLM settings. For each target token (detailed in Sections A.2 and A.3), we compare its grounding information gain with

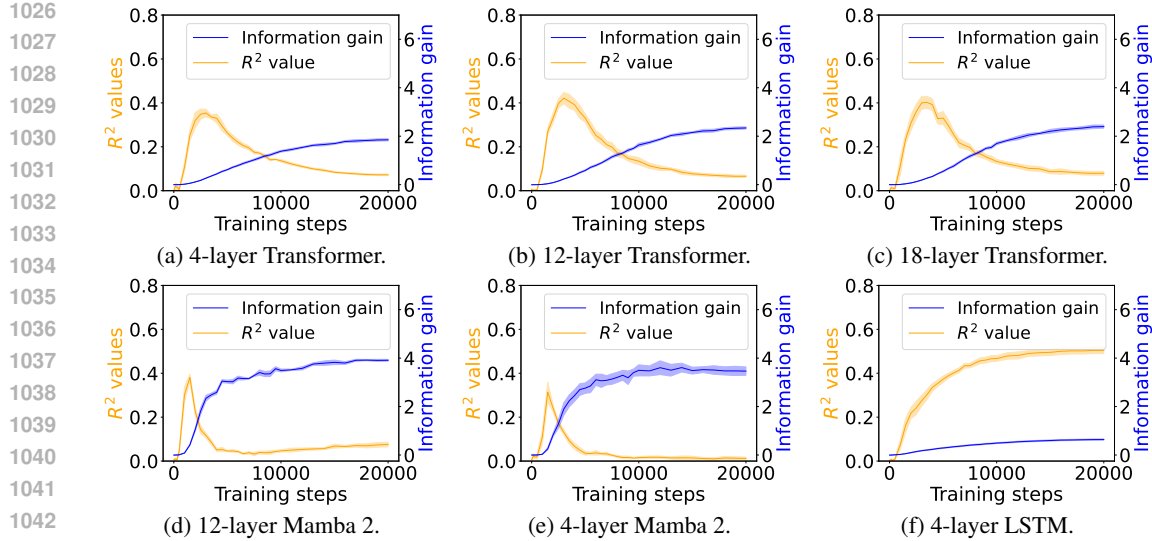


Figure 9: Grounding information gain and its correlation to the co-occurrence of linguistic and environment tokens over training steps.

the average aggregate head it has (Figure 12). We find an intermediate-to-strong positive correlation between the grounding information gain and the aggregate head number detected.

D LLM STATEMENT

In this work, large language models (LLMs) are employed in two limited ways: (i) to polish the writing and improve the linguistic clarity of the paper; (ii) to assist in code writing and debugging. LLMs are not involved in the design of the core method, the experimental setup, data analysis, or the interpretation of the results. All texts presented in the paper, as well as the code, are endorsed by the authors, and the authors take full responsibility of the content presented in this paper.

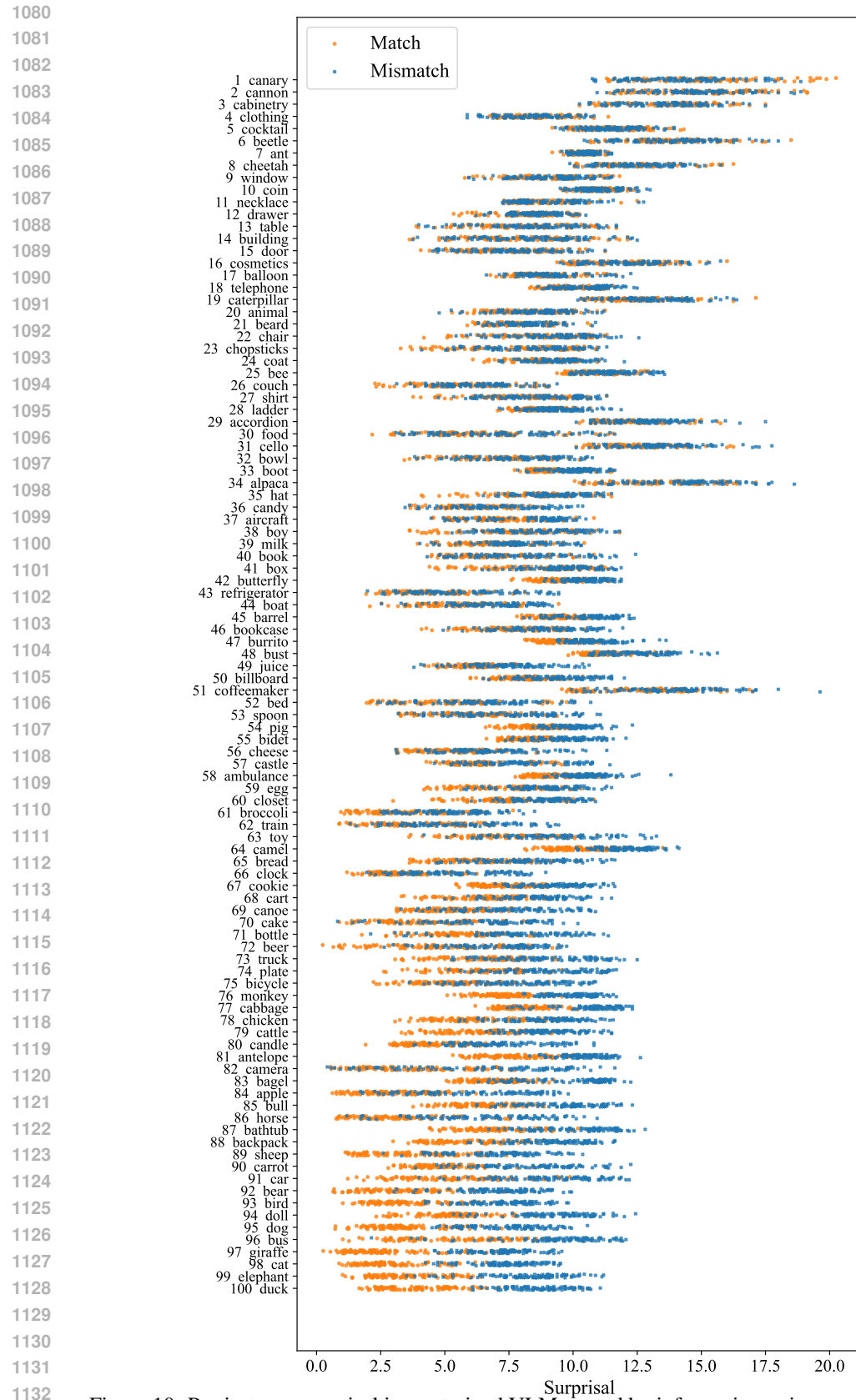


Figure 10: Per-instance surprisal in our trained VLM, sorted by information-gain per word (increasing). Orange dots: surprisals in matched context; blue cross: surprisals in mismatched context.

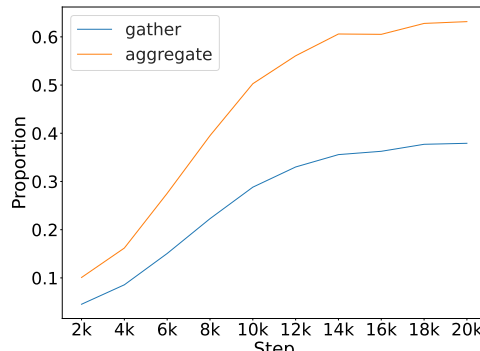


Figure 11: Gather-and-aggregate overtime strength.

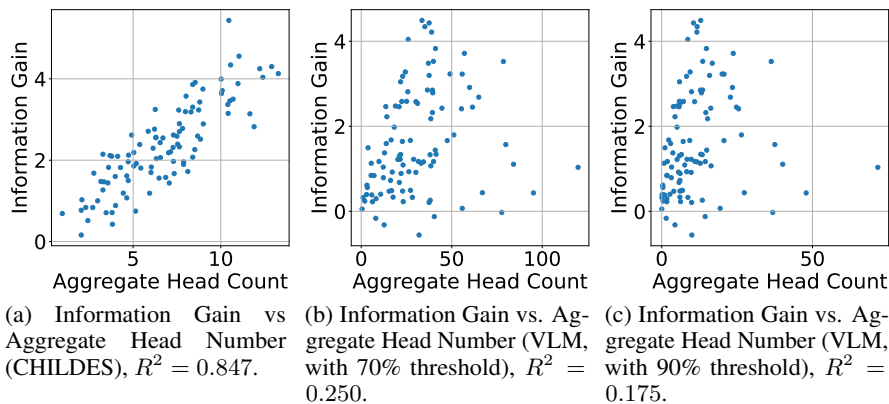


Figure 12: Grounding information gain vs. number of aggregate heads.